Monthly Notices
of the
ROYAL ASTRONOMICAL SOCIETY

MNRAS **445,** 3908–3918 (2014) doi:10.1093/mnras/stu2059

Spectroscopy of Hyades L dwarf candidates⋆

N. Lodieu,[1,2]† S. Boudreault[1,2,3] and V. J. S. Béjar[1,2]

[1]*Instituto de Astrofísica de Canarias (IAC), C/ Vía Láctea s/n, E-38200 La Laguna, Tenerife, Spain*
[2]*Departamento de Astrofísica, Universidad de La Laguna (ULL), E-38206 La Laguna, Tenerife, Spain*
[3]*GEPI, Observatoire de Paris, CNRS, Université Paris Diderot; 5 Place Jules Janssen, F-92190 Meudon, France*

Accepted 2014 September 29. Received 2014 September 15; in original form 2014 July 30

ABSTRACT

We present the results of photometric, astrometric, and spectroscopic follow-up of L dwarf candidates identified in the Hyades cluster by Hogan et al. We obtained low-resolution optical spectroscopy with the Optical System for Imaging and low-intermediate Resolution Integrated Spectroscopy spectrograph on the Gran Telescopio de Canarias for all 12 L dwarf candidates as well as new *J*-band imaging for a subsample of 8 to confirm their proper motion. We also present mid-infrared photometry from the *Wide Field Infrared Survey Explorer* for the Hyades L and T dwarf candidates and estimate their spectroscopic distances, effective temperatures, and masses. We confirm the cool nature of several L dwarf candidates and confirm astrometrically their membership, bridging the gap between the coolest M dwarfs and the two T dwarfs previously reported in the Hyades cluster. These members represent valuable spectral templates at an age of 625 Myr and slightly supersolar metallicity (Fe/H = +0.13). We update the Hyades mass function across the hydrogen-burning limit and in the substellar regime. We confirm a small number numbers of very low mass members below ∼0.1 $M_{\odot}$ belonging to the Hyades cluster.

Key words: techniques: photometric – techniques: spectroscopic – astronomical data bases: catalogues – brown dwarfs – Infrared: stars.

1 INTRODUCTION

The shape of the initial mass function (IMF) is of prime importance to understand the processes responsible for the formation of stars and brown dwarfs. The form of the IMF across the stellar/substellar limit is of particular interest to assess whether stars and brown dwarfs represent two distinctive populations (Thies & Kroupa 2007, 2008) or have properties differing due to dynamical interactions (Parker & Andersen 2014). The definition and first estimate of the IMF was presented by Salpeter (1955) and updated by Miller & Scalo (1979) and Scalo (1986). Our current knowledge of the IMF suggests that it is best fitted by a lognormal form (Chabrier 2003, 2005) or a combination of power laws (Kroupa 2002; Kroupa et al. 2013), with little variations across a large range of masses and environments (see review by Bastian, Covey & Meyer 2010). Studying the form and shape of the bottom-end of the mass function in relatively old clusters like the Hyades, where low-mass members may have been evaporated by dynamical evolution, is of interest to study the intrinsic evolution of individual brown dwarfs and how the stellar and substellar populations evolve. Looking at the shape of the IMF at different metallicities is also important to probe its dependence with environment.

The Hyades cluster has a mean distance of 46.3 ± 0.3 pc, a significant proper motion ranging between 74 and 140 mas yr^{-1}, a tidal radius of ∼10 pc, and a core radius of 2.5–3.0 pc, according to the analysis of the *Hipparcos* catalogue by Perryman et al. (1998). The age of the cluster is estimated to be 625 ± 50 Myr based on reproducing the observed cluster sequence with model isochrones which include convective overshooting (Maeder & Mermilliod 1981), although a larger range in age cannot be discarded (Eggen 1998). The metallicity of the Hyades high-mass stars appears slightly supersolar, with values between 0.127 ± 0.022 and 0.14 ± 0.1 (Boesgaard & Friel 1990; Cayrel de Strobel, Crifo & Lebreton 1997; Grenon 2000), although a more recent work by Gebran et al. (2010) suggests a mean metallicity close to solar ([Fe/H] = 0.05 ± 0.05). Despite being one of the closest and best studied open cluster, the Hyades still hold secrets regarding its membership, dynamics, and evolution. The majority of surveys have focused on small patches of the sky near the cluster centre to identify new members (Hanson 1975; Leggett & Hawkins 1989; Reid 1993; Stauffer et al. 1994; Stauffer, Liebert & Giampapa 1995; Reid & Gizis 1997; Reid & Hawley 1999; Dobbie et al. 2002). Some larger area surveys have been undertaken in the past (e.g. Reid 1992), recently updated by

⋆Based on observations collected with telescopes operated on the island of La Palma in the Spanish Observatorio del Roque de los Muchachos of the Instituto de Astrofísica de Canarias.

† E-mail: nlodieu@iac.es

the study of Röser et al. (2011) using the PPMXL catalogue (Röser, Demleitner & Schilbach 2010). However, this search was limited in magnitude to $V \sim 20$ mag, yielding a catalogue of 364 stars within the tidal radius of the cluster, down to 0.2 $M_\odot$ corresponding to a spectral type of M4. This work was recently extended by Goldman et al. (2013) down to lower masses (~0.09 $M_\odot$) by combining PPMXL with PanStarrs (Kaiser et al. 2002) to derive the cluster mass function in the low-mass regime. Gizis, Reid & Monet (1999) attempted to select photometrically L dwarf candidates in the Hyades from a photometric search in the Two Micron All Sky Survey (2MASS; Cutri et al. 2003; Skrutskie et al. 2006) but did not confirm any of the candidate as spectroscopic member. Hogan et al. (2008) conducted a similar photometric and astrometric work cross-correlating 2MASS and the UKIRT Infrared Deep Sky Survey (UKIDSS; Lawrence et al. 2007) Galactic Clusters Survey (GCS), yielding a sample of 12 L dwarf candidates, four of them recently confirmed as ultracool dwarfs by near-IR spectroscopy (Casewell et al. 2014). At the low-mass end of the mass function, Bouvier et al. (2008) identified spectroscopically the first two T dwarfs in the Hyades, with masses estimated to ~0.05 $M_\odot$ according to theoretical isochrones (Baraffe et al. 1998; Chabrier et al. 2000).

In this paper, we present an astrometric, photometric, and spectroscopic follow-up of L dwarf candidates in the Hyades open cluster published by Hogan et al. (2008) to assess their membership. In Section 2, we describe the photometric observations and its associated data reduction. In Section 3, we present the optical spectroscopy carried out with the Gran Telescopio de Canarias (GTC). In Section 4, we derive the spectral types of the Hyades candidates presented in Hogan et al. (2008) and discuss their membership based on our photometric, astrometric, and spectroscopic observations. In Section 5, we derive physical properties of the confirmed L dwarfs, including spectroscopic distances, effective temperatures, and masses based on state-of-the-art models. In Section 6, we discuss the shape of the luminosity and mass functions and compare them to the Praesepe cluster whose age is comparable to the Hyades.

2 PHOTOMETRIC AND ASTROMETRIC FOLLOW-UP

2.1 Near-infrared imaging

We conducted *J*-band imaging follow-up with the Long-slit Intermediate Resolution Infrared Spectrograph (LIRIS; Manchado et al. 1998) at the Cassegrain of the William Herschel Telescope (WHT) located on the Observatorio del Roque de Los Muchachos en La Palma (Canary Islands). We carried out this project on 2014 January 13 as a back-up programme during an unrelated run due to the poor transparency (thin clouds passing by) and variable seeing poorer than 1.3 arcsec because of the brightness of the Hyades targets. We observed 8 of the 12 L dwarf candidates of Hogan et al. (2008): Hya03–08, Hya10, and Hya12.

LIRIS is equipped with a 1024 × 1024 pixel HAWAII detector sensitive to near-infrared wavelengths (0.8–2.5 μm) with a pixel scale of 0.25 arcsec, giving a field of view of 4.7 by 4.7 arcmin across. The instrument is equipped with a large set of filters, including the *J* broad-band filter used for our photometric follow-up. We employed a nine-point dithering pattern with on-source individual integrations of 5 s repeated one or twice with a small jitter offset, yielding a total on-source integration of 5 or 10 min. We obtained dome flats during the afternoon preceding the observations. We did not observe any photometric standard stars because our fields are covered by 2MASS, providing us with magnitudes calibrated to the 2MASS system. We will use these observations to complement the *K*-band photometry of UKIDSS and provide an additional epoch to the 2MASS and UKIDSS epochs.

2.2 Data reduction

We carried out the data reduction of the LIRIS images on the fly on the mountain with the LIRIS pipeline.[1] This procedure is fairly automatized and consists of subtracting the sky made from the dithered images to each individual image of the target. The pipeline also includes a correction for flat-field (median image made of the median dome flats taken during the afternoon), vertical gradient observed on the detector, and the geometrical distortion. The corrected images obtained per object are then aligned and combined to provide a final image taking into account the random offsets between the dithered and jittered positions.

The pipeline-reduced combined images include a rough astrometric calibration, but there is a significant offset (~20 arcsec) with the world coordinate system. To obtain an accurate astrometric calibration of the LIRIS images, we have made use of the Graphical Astronomy and Image Analysis Tool (GAIA).[2] We employed the astrometric facility under the image analysis tool by tweaking the existing calibrations of the UKIDSS GCS (Lawrence et al. 2007). We shifted all UKIDSS GCS detections brighter than $K = 17.8$ mag to their positions on the LIRIS images and removed objects lying on the edge of the detector to optimize the six-parameter polynomial fit (of the order of 2) of the astrometric solution. We obtained rms errors on the astrometric fit of 0.63–0.93 pixel, i.e. 0.16–0.23 arcsec, based on samples of a few tens of stars.

We used the aforementioned astrometrically-calibrated images to derive the photometry. We derived instrumental magnitudes using the photometric analysis tools in GAIA, which makes use of SEXTRACTOR (Bertin & Arnouts 1996). We employed a fixed aperture radius of 8 pixels (= 2 arcsec) for all images, slightly larger than the full width at half-maximum which oscillated between 1.2 and 1.9 arcsec during the observations of the Hyades cluster members. We inferred photometric zero-points for each LIRIS image from point sources brighter than $J_{2MASS} = 15.9$ mag, equivalent to a 10σ detection in 2MASS. We point out that this process cannot be carried out with the UKIDSS GCS catalogue because only *K*-band photometry is available towards the Hyades cluster. This limit in magnitude yielded photometric zero-points in the 22.398–23.024 mag range with uncertainties less than 6 per cent, based on 5 to 23 stars in the LIRIS field of view. We list the final *J*-band magnitudes of Hya03–08, Hya10, and Hya12 and the details of the observations in Table 1. We find good agreement with the 2MASS magnitudes quoted by Hogan et al. (2008) within the photometric uncertainties.

3 OPTICAL SPECTROSCOPY

3.1 Spectroscopic observations

We obtained low-resolution ($R \sim 200$ or 400) optical spectroscopy with the OSIRIS (Optical System for Imaging and low-intermediate Resolution Integrated Spectroscopy; Cepa et al. 2000) mounted on the 10.4-m GTC telescope in La Palma over several nights. OSIRIS is equipped with two 2048 × 4096 Marconi CCD42-82 detectors offering a field of view approximately 7 arcmin × 7 arcmin with

[1] www.ing.iac.es/Astronomy/instruments/liris/liris_ql.html
[2] http://star-www.dur.ac.uk/~pdraper/gaia/gaia.html

Table 1. log of the WHT LIRIS and GTC OSIRIS photometric and spectroscopic observations for the Hyades L dwarf candidates published by Hogan et al. (2008). Coordinates are from our LIRIS observations taken on 2014 January 13 (in J2000), except for the four candidates not observed photometrically which are taken from Hogan et al. (2008). 'Nb' stands for the numbers of exposures at a given position.

ID	RA	Dec.	Photometry						Spectroscopy				
			Tel/Instr.	Date	ExpT	Nb	Seeing	J (errJ)	Tel/Instr.	Date	ExpT	Nb	Grism
	(hh:mm:ss.ss)	(°:′:″)		(ddmmyyyy)	(s)		(arcsec)	(mag)		(ddmmyyyy)	(s)		
Hya01	04:20:24.50	+23:56:13.0	–	–	–	–	–	–	GTC OSIRIS	23102013	600	1	R500R	M8.5
Hya02	03:52:46.30	+21:12:33.0	–	–	–	–	–	–	GTC OSIRIS	25102013	600	1	R300R	L1.5
Hya03	04:10:24.01	+14:59:10.3	WHT LIRIS	13012014	10	18	1.3	15.647 (0.076)	GTC OSIRIS	16102013	300	1	R500R	L0.5
Hya04	04:42:18.59	+17:54:37.3	WHT LIRIS	13012014	10	18	1.5	15.595 (0.044)	GTC OSIRIS	16102013	300	1	R500R	M9.5
Hya05	03:58:43.06	+10:39:39.6	WHT LIRIS	13012014	10	18	1.4	15.729 (0.071)	GTC OSIRIS	16102013	300	1	R500R	M5
Hya06	04:22:05.22	+13:58:47.3	WHT LIRIS	13012014	10	18	1.7	15.462 (0.081)	GTC OSIRIS	16102013	300	1	R500R	M9.5
Hya07	04:39:29.17	+19:57:34.6	WHT LIRIS	13012014	10	18	1.8	15.956 (0.073)	GTC OSIRIS	16102013	300	1	R500R	M3
Hya08	04:58:45.75	+12:12:34.1	WHT LIRIS	13012014	10	18	1.3	15.463 (0.044)	GTC OSIRIS	16102013	300	1	R500R	L0.5
Hya09	04:46:35.40	+14:51:26.0	–	–	–	–	–	–	GTC OSIRIS	22032014	1800	1	R500R	L2.0
Hya10	04:17:33.97	+14:30:15.4	WHT LIRIS	13012014	10	18	1.4	16.506 (0.059)	GTC OSIRIS	26102013	600	4	R300R	L1.0
Hya11	03:55:42.00	+22:57:01.0	–	–	–	–	–	–	GTC OSIRIS	23102013	600	1	R500R	L1.5
Hya12	04:35:43.02	+13:23:44.8	WHT LIRIS	13012014	10	18	1.3	16.778 (0.069)	GTC OSIRIS	26102013	600	4	R300R	L3.5

an unbinned pixel scale of 0.125 arcsec. We observed the Hyades L dwarf candidates as part of a run in visitor mode (GTC27-13B) and two filler programmes in service mode (GTC65-13B; GTC5-14A; PI Lodieu). We observed three L dwarf candidates Hya02, Hya10, and Hya12 during our visitor mode run as back-up targets due to the poor transparency and bad seeing conditions. We took spectra for the remaining nine L dwarf candidates under variable conditions as part of our filler programmes, which accepts seeing worse than 1.5 arcsec, bright time, and cirrus. The slit was set to 1 or 1.5 arcsec depending on the seeing. The log of the observations is in Table 1. We observed the spectrophotometric standards, G191-B2B (van Leeuwen 2007; Gianninas, Bergeron & Ruiz 2011) and Hilt 600 (Høg et al. 2000; Pancino et al. 2012) with both gratings. We obtained an additional spectrum of the standards with the Z filter to correct for the second-order contamination beyond 9000 Å which affects those low-resolution gratings (see also Zapatero Osorio et al. 2014). Bias frames, dome flat-fields, and neon, xenon, and HgAr arc lamps were observed by the observatory staff during the afternoon preceding the observations.

We have also made use of optical spectral templates of M8–L4 dwarfs taken with GTC OSIRIS taken as part of programmes GTC66-12B and GTC62-13B (PI Boudreault). We used the grism R300R and a slit of 1 arcsec with a single on-source integration between 300 and 900 s scaled according to the magnitude. We emphasize that the settings used for these spectral templates closely resembles the ones used for the Hyades targets, yielding similar spectral resolution. We considered the following field M and L dwarfs classified in the optical: LP 213-68 (M8; Reid et al. 2002), 2MASS J02512220+2521236 (M9; Hawley et al. 2002) 2MASP J0345432+254023 (L0; Kirkpatrick, Beichman & Skrutskie 1997; Kirkpatrick et al. 1999; Dahn et al. 2002; Knapp et al. 2004), SDSS J163050.01+005101.3 (L1; Hawley et al. 2002; Jameson et al. 2008), 2MASSW J0030438+313932 (L2; Kirkpatrick et al. 1999; Jameson et al. 2008), 2MASSW J0355419+225702 (L3; Kirkpatrick et al. 1999), and 2MASSW J1155009+230706 (L4; Kirkpatrick et al. 1999; Jameson et al. 2008).

3.2 Data reduction

We reduced the OSIRIS optical spectrum following a standard methodology under the IRAF environment (Tody 1986, 1993). We subtracted the raw spectrum by a median-combined bias and divided by a normalized median-combined dome flat-field taken during the afternoon. We extracted optimally a 1D spectrum from the 2D image and calibrated that spectrum in wavelength with the lines from the combined arc lamp. We calibrated the spectra of the Hyades in flux with the spectrophotometric standard corrected for the second-order contamination. The spectral templates, which were taken prior to summer 2013, were observed solely with the grating and without the Z filter, hence, were not corrected for the second-order contamination. As a consequence, the flux calibration of these spectral standards is only trustworthy up to 900 nm. We combined the template spectra to create references for each half subtype (L0.5, L1.5, L2.5, and L3.5). The GTC spectra for 12 Hyades L dwarf candidates, normalized at 7500 Å, are displayed in Fig. 1.

4 MEMBERSHIP OF L DWARF CANDIDATES

4.1 Photometric membership

Hogan et al. (2008) selected 12 L dwarf candidates photometrically and astrometrically. We obtained J-band photometry for 8 of these

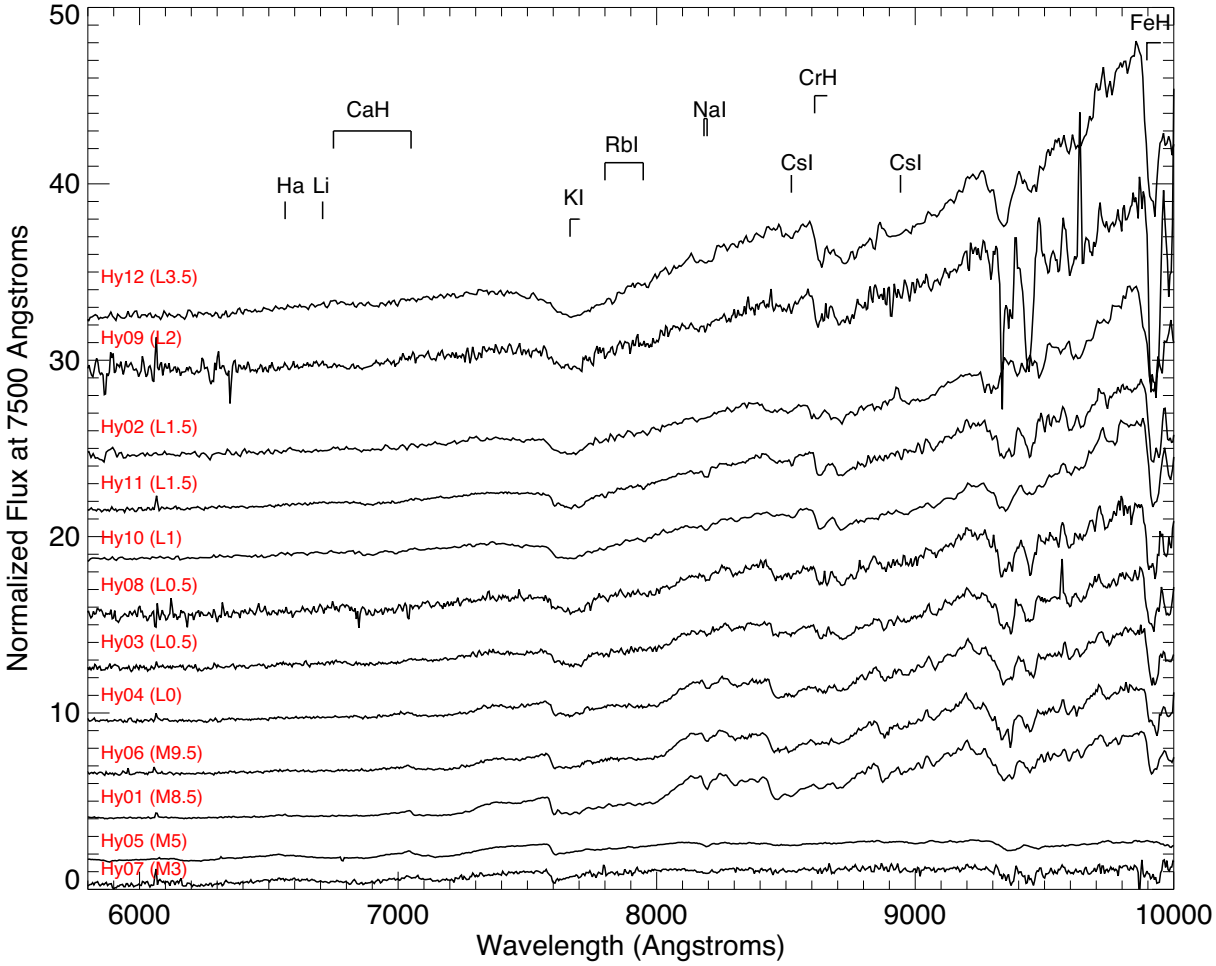

Figure 1. Low-resolution optical spectra for 12 Hyades L dwarf candidates from Hogan et al. (2008) obtained with the R300R and R500R gratings on the GTC/OSIRIS spectrograph. Some important absorption bands and atomic lines affecting the spectral energy distribution of M and L dwarfs are labelled .

12 L dwarfs (Hya03–08, Hya10, and Hya12) and confirmed their magnitudes compared to 2MASS within the photometric errors. In Fig. 2, we plot the $(J - K_s, J)$ colour–magnitude depicting known Hyades members Goldman et al. (2013) along with the 12 L dwarf candidates (dots with their associated identification number) and the two T dwarfs (open triangles; Bouvier et al. 2008). We overplotted the 600 Myr isochrones from the BT-Settl models (Allard, Homeier & Freytag 2012) as well as ultracool dwarfs with parallaxes from Dupuy & Liu (2012). We note that we removed subdwarfs from their list. We can see that the L dwarf candidates bridge the gap between Hyades M and T dwarfs, adding credit to their membership.

4.2 Astrometric membership

To carry out the proper motion analysis, we made use of UKIDSS images as first epoch (images typically taken between 2005 October 9 and December 27) and LIRIS images as a second epoch. These data provide a baseline of about 8 yr. For Hya02 and Hya11, we made use of two epochs of UKIDSS separated by about 5 yr for the proper motion determination because we did not obtain LIRIS imaging. We estimated the proper motion by comparison of the relative positions of the targets with respect to about 15–30 reference stars located in a field of 4 arcmin by 4 arcmin around the candidate position. We used the GEOMAP routine within the IRAF environment to convert pixel coordinates from the first to the second epoch. We employed a general transformation with a polynomial function of the order of 3. We converted the resulting pixel displacements of our targets into proper motions using the astrometric solution given by the UKIDSS images. We estimate the uncertainties in the proper motion by summing quadratically the errors in the centroids, which are of the order of 1/3 and 1/30 of pixel in the LIRIS and UKIDSS images, respectively, and the standard deviation of the transformation of reference stars. We indicate the resulting proper motions and their uncertainties in Table 2. The mean proper motion of the L dwarf candidates is $(\mu_\alpha \cos\delta, \mu_\delta) = (106.10, -19.35)$ mas yr^{-1} with an intrinsic dispersion (after removing proper motion errors) of 25.5 mas yr^{-1} and 7.4 mas yr^{-1} in right ascension and declination, respectively (total is 26.5 mas yr^{-1}). For comparison, the total intrinsic dispersion of Hyades members from Goldman et al. (2013) in the area covered by Hogan et al. (2008) with masses in the 2.6–2.0, 2.0–1.0, 1.0–0.5, and 0.5–0.2 $M_\odot$ are 17.96, 19.67, 23.82, and 26.89 mas yr^{-1}, respectively.

In Fig. 3, we plot the measured proper motions of the eight L dwarf candidates (black dots) observed with WHT/LIRIS in a vector point diagram to further assess their membership. We overplotted in that figure the known Hyades members published by Goldman et al. (2013) with small grey crosses. We can observe the large dispersion of the members, centred around (100,−25) mas yr^{-1}. We also added the proper motions measured for point sources lying in the LIRIS fields of view (blue open squares). On the one hand, we

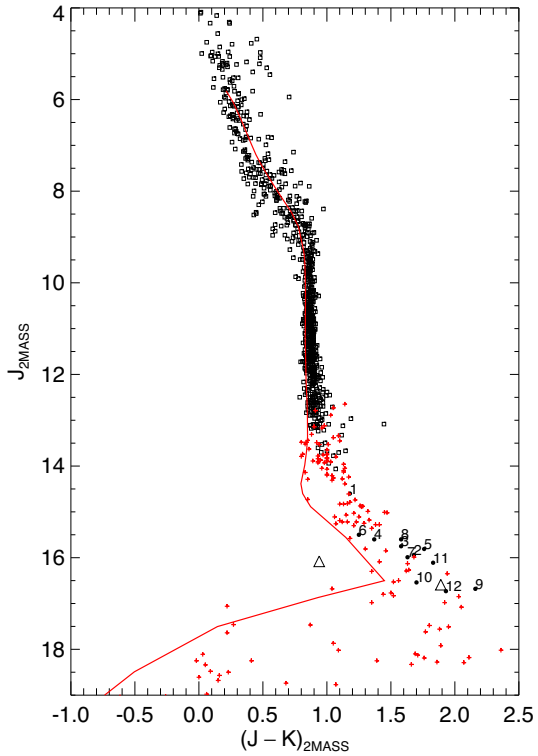

Figure 2. ($J - K_s$, J) colour–magnitude diagram for known Hyades stellar members from Goldman et al. (2013) marked as open squares. Overplotted are the 12 L dwarf candidates (filled circles with ID numbers) from Hogan et al. (2008). Candidates numbers 5 and 7 are rejected as members by our spectroscopic follow-up. For completeness, we added the two T dwarfs confirmed spectroscopically by Bouvier et al. (2008) as open triangles. Overplotted as red crosses are ultracool dwarfs with parallaxes from Dupuy & Liu (2012) as well as the 600 Myr BT-Settl isochrone (red line) shifted at the distance of the Hyades.

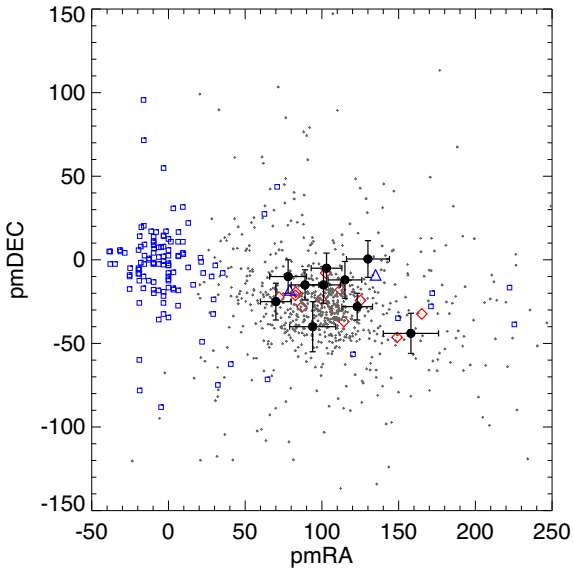

Figure 3. Vector point diagram for Hyades L dwarf candidates. Large filled dots are proper motions with their associated error bars derived from the LIRIS versus UKIDSS GCS DR10 cross-match presented in this paper, while large red open diamonds are measurements from Hogan et al. (2008). Small open blue square represents the dispersion of all point sources in the LIRIS fields. Overplotted as grey symbols are all Hyades members from Goldman et al. (2013). T dwarfs from Bouvier et al. (2008) are displayed as large blue open triangles.

confirm that most objects lie around (0,0) in the vector point diagram, except for several cases which we cannot discard as members of the Hyades. On the other hand, we estimate a mean astrometric error representing the quadratic sum of the centroid errors and standard deviation of the order of 15 mas yr^{-1}, based on the dispersion of the open squares.

Table 2. Near- and mid-infrared photometry, proper motions (in mas yr^{-1}), spectral types with half a subclass uncertainty, spectroscopic distances (in pc) based on the *J*-band photometry, effective temperatures (in kelvins) using field L dwarfs with parallax measurements (Dahn et al. 2002; Vrba et al. 2004), masses (in $M_\odot$) from the BT-Settl models (Allard et al. 2012), and final membership assignment (Memb?) for the 12 Hyades L dwarf candidates identified by Hogan et al. (2008). The bottom panels list the same data sets but for the two T dwarfs in Bouvier et al. (2008). Note: Hya02 is a blend in *WISE* images. The *WISE* photometry of Hya04 and Hya10 is most likely affected by the contribution of a faint sources seen on the UKIDSS GCS *K*-band images within the spatial resolution of *WISE*.

ID	$J_{\rm LIRIS}$ (mag)	$w1$ (mag)	$w2$ (mag)	$\mu_\alpha \cos\delta$ (mas yr^{-1})	μ_δ (mas yr^{-1})	d (pc)	SpT	$T_{\rm eff}$ (K)	Mass ($M_\odot$)	Memb?
Hya01	–(–)	13.087 (0.024)	12.846 (0.030)	–	–	$48.9^{+3.8}_{-3.4}$	M8.5	2379 (82)	0.071–0.080	Yes
Hya02	–(–)	13.582 (0.026)	13.276 (0.032)	123 ± 10	-28 ± 8	$57.7^{+4.9}_{-5.0}$	L1.5	2332 (114)	0.068–0.079	Y?
Hya03	15.647 (0.076)	13.948 (0.029)	13.695 (0.036)	103 ± 10	-5 ± 9	$62.1^{+4.7}_{-4.9}$	L0.5	2320 (133)	0.069–0.079	Yes
Hya04	15.595 (0.044)	13.819 (0.026)	13.601 (0.035)	70 ± 10	-25 ± 11	$67.1^{+4.7}_{-4.9}$	M9.5	2421 (185)	0.073–0.097	Yes
Hya05	15.729 (0.071)	13.447 (0.025)	13.058 (0.028)	130 ± 15	$+1.0 \pm 11$	$173.1^{+4.0}_{-53.0}$	M5.0	– (–)	–	No
Hya06	15.462 (0.081)	13.928 (0.028)	13.639 (0.038)	78 ± 12	-10 ± 10	$64.3^{+4.5}_{-4.7}$	M9.5	2421 (185)	0.073–0.097	Yes
Hya07	15.956 (0.073)	13.486 (0.026)	13.277 (0.032)	94 ± 15	-40 ± 15	$443.8^{+51.3}_{-115.7}$	M3.0	– (–)	–	No
Hya08	15.463 (0.044)	13.718 (0.026)	13.494 (0.033)	89 ± 9	-15 ± 9	$57.9^{+4.4}_{-4.6}$	L0.5	2320 (133)	0.069–0.079	Yes
Hya09	–(–)	13.942 (0.028)	13.563 (0.034)	–	–	$73.2^{+5.5}_{-7.9}$	L2.0	2368 (198)	0.066–0.085	Y?
Hya10	16.506 (0.059)	12.857 (0.024)	12.791 (0.027)	115 ± 11	-12 ± 11	$82.6^{+6.8}_{-6.6}$	L1.0	2295 (82)	0.068–0.075	Y?
Hya11	–(–)	13.641 (0.025)	13.311 (0.032)	158 ± 18	-44 ± 12	$62.4^{+6.0}_{-5.4}$	L1.5	2332 (114)	0.068–0.079	Y?
Hya12	16.778 (0.069)	14.226 (0.028)	13.804 (0.047)	101 ± 11	-15 ± 11	$57.3^{+5.3}_{-5.8}$	L3.5	1982 (114)	0.054–0.063	Y?
Hya20	–(–)	15.597 (0.048)	14.722 (0.078)	–	–	$28.8^{+0.3}_{-0.3}$	T2.0	1361 (150)	0.030–0.040	Y?
Hya21	–(–)	15.280 (0.041)	14.830 (0.100)	–	–	$55.5^{+0.4}_{-0.1}$	T1.0	1288 (150)	0.030–0.040	Yes

Moreover, we confirm the proper motions published in table 2 of Hogan et al. (2008). Overall, we conclude that the eight L dwarf candidates followed-up photometrically with LIRIS have a proper motion consistent with more massive members of the Hyades cluster.

4.3 Spectroscopic membership

We have investigated further the nature of the 12 L dwarf candidates with our GTC/OSIRIS spectroscopic follow-up. To assign the spectral types to our candidates, we opted for the direct comparison with spectral templates. For spectral types earlier than (or equal to) L0 (Hya01, Hya04, Hya05, and Hya07), we made use of the Sloan Digital Sky Survey (SDSS; York et al. 2000) spectroscopic data base (Bochanski et al. 2007). This data base contains a repository of good-quality M0–L0 spectra spanning the 380–940 nm wavelength range at a resolution of 2000. All spectra are wavelength- and flux-calibrated and corrected for telluric absorption. M dwarfs are classified based on the Hammer classification scheme (Covey et al. 2007) which uses the spectral energy distribution of stars over the 0.3–2.5 μm range using photometry from SDSS and 2MASS. We added subtypes to this list of templates to provide a complete list of spectral templates with optical spectral types accurate to one subtype.

For spectral types later than L0 (Hya02–03, Hya08–12), we employed spectral templates observed with GTC OSIRIS at a similar spectral resolution for direct comparison (Section 3.1). We have spectral templates for each half subtype, from L0 up to L4. We note that the GTC optical spectra of our M8, M9, and L0 spectral templates agree closely with the Sloan templates. Our uncertainty on the spectral types is 0.5 subtype.

Casewell et al. (2014) derived spectral types for five candidates in common to our work, based on low-resolution near-infrared spectra. They rejected Hya02 as a Hyades members whereas we can clearly see that its spectrum looks like an L dwarf with a spectral type of L0.5 (Fig. 1). We classify two objects (Hya01 and Hya04) roughly two spectral types earlier than Casewell et al. (2014), M8.5 versus L0.5 and L0 versus L2–L3, respectively. Our uncertainty on the spectral type is lower than the ones from the near-infrared classification of Casewell et al. (2014). This trend of earlier spectral types derived from optical spectra versus near-infrared spectra has already been seen in young dwarfs (e.g. Lodieu et al. 2005). Our spectral types for Hya03 and Hya06 agree with those of Casewell et al. (2014), L0.5 versus M8–L0.5 and M9.5 versus M8–L2, but our uncertainty on the spectral type is accurate to half a subclass, better than the near-infrared spectral types of Casewell et al. (2014).

To summarize, we found 2 M dwarf contaminants (Hya05 and Hya07), 3 late-M dwarfs (Hya01, Hya04, and Hya06), and 7 L dwarfs (spectral types between L0 and L3.5) among the 12 candidates reported in Hogan et al. (2008). Hence, the success rate of the technique employed by Hogan et al. (2008) to identify L dwarfs in the Hyades is larger than 58 per cent. Hogan et al. (2008) predicted 2 contaminants (photometric and proper motion non-members) out of the 12 candidates, estimate confirmed by the presence of 2 early-M dwarfs in the sample.

4.4 *WISE* mid-infrared photometry

We have also downloaded the *Wide Field Infrared Survey Explorer* (*WISE*) all-sky photometry (Wright et al. 2010) to further assess the membership of these 12 L dwarf candidates. *WISE* observed the full sky in four mid-infrared filters centred at 3.4, 4.6, 12, and 22 μm down to 5σ limits of 16.5, 15.5, 11.3, and 7.9 mag (Vega system) with spatial resolutions of 6.1, 6.4, 6.5, and 12 arcsec, respectively. We checked the *WISE* images where all candidates are detected in $w1$ and $w2$ with signal-to-noise ratios in the 37–45 and 23–40, respectively. However, none of the L dwarfs are detected in the $w3$ and $w4$ bands (Table 2). We also downloaded the *WISE* photometry for the two T dwarfs, where the signal-to-noise ratios in $w1$ and $w2$ are 22–26 and 10–14, respectively. As for the L dwarfs, the T dwarfs are undetected in the other *WISE* passbands. The $K - w2$ and $J - w1$ colours of CFHT-Hy-20 (T2) and CFHT-Hy-21 (T1) are consistent with the typical colours of field late-L and early-T dwarfs as depicted in Fig. 4. We should mention that there is a faint nearby source on the GCS *K*-band image, which likely affects the *WISE* photometry of CFHT-Hy-21.

In Fig. 4, we display the ($J - w1$, J) and ($K_s - w2$, K_s) colour–magnitude diagrams for known members of the Hyades (open squares; Goldman et al. 2013) to which we added the Hyades L and T dwarfs and field ultracool dwarfs with parallaxes (Dupuy & Liu 2012). We observe 2 subgroups among the 12 L dwarf candidates. We find six candidates that lie below the Hyades sequence of low-mass stars and seem to bridge the gap with the Hyades T dwarfs. This group contains three late-M dwarfs (Hya01, Hya04, and Hya06) and three L dwarfs (Hya03, Hya08, and Hya10). These objects also fit the sequence of spectral types for ultracool dwarfs with parallaxes (red crosses in Fig. 4), which is not too surprising because the age of the Hyades is close to the mean age of field dwarfs.

The group showing the reddest colours in $J - w1$ and $K_s - w2$ (Fig. 4) includes two spectroscopic non-members (Hya05 and Hya07; see Section 4.3) and Hya02 which has a companion on the UKIDSS GCS *K*-band image unresolved on the *WISE* images due to its poorer spatial resolution at 3.6 and 4.5 μm (∼6.5 arcsec; Wright et al. 2010). For this reason, we urge caution in the interpretation its magnitudes and colours. The other three sources in this 'red' group are Hya09, Hya11, and Hya12, which we classify as L dwarfs (Table 2; Section 4.3). One of them, Hya11, has a position in the sky very close to the Pleiades (Fig. 5) and is reported as a non-member in table A1 of Lodieu, Deacon & Hambly (2012b) because of its large proper motion ($\mu_\alpha cos\delta = 161.1 \pm 2.3$ and $\mu_\delta = -44.5 \pm 2.3$ mas yr^{-1}), which is consistent with the Hyades proper motion. Casewell, Jameson & Burleigh (2008) and Faherty et al. (2009) reported proper motions of (172,−21) mas yr^{-1} and (142,−25) mas yr^{-1} for Hya11, respectively. We also note that no companion was detected around Hya11 down to magnitude limits of $J = 20.5$ mag and $K = 18.5$ mag with separations in the 2–31 arcsec range (Allen et al. 2007). The other two sources remain with mid-infrared excess and could be younger than the Hyades but we do not detect Hα in emission or see obvious signs of youth (e.g. weaker atomic lines) at the resolution of our spectra. None the less, we cannot discard at this stage that these mid-IR excesses characteristics of youth may extent to the typical age of the Hyades and hence, could be used as a criterion to confirm their membership.

5 PHYSICAL PROPERTIES OF HYADES L DWARF CANDIDATES

5.1 Spectroscopic distances

To further assess the likelihood of the new late-M and L dwarfs to belong to the Hyades cluster, we have computed spectroscopic distances based on the *J*-band absolute magnitude versus spectral type relationship from Dupuy & Liu (2012), which is valid for field

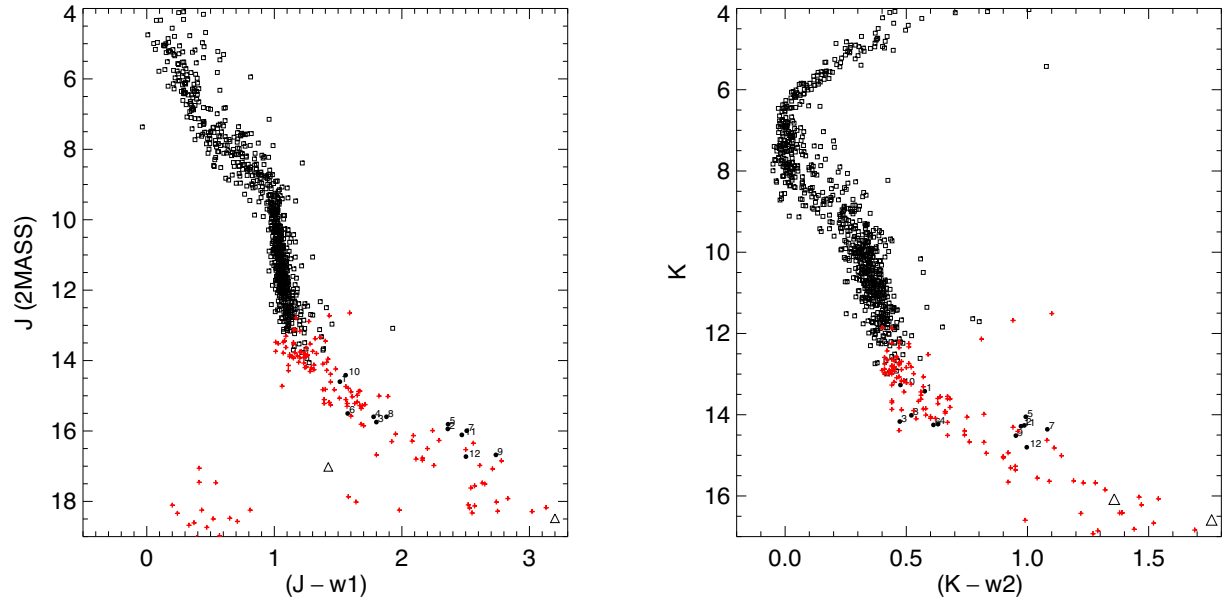

Figure 4. $(J - w1, K)$ and $(K_s - w2, K_s)$ colour–magnitude diagrams for known Hyades stellar members (open squares; Goldman et al. 2013) and candidates from Hogan et al. (2008) with optical spectra (dots marked with numbers following the order in Table 1). Candidates Hya05 and Hya07 are rejected as members whereas the *WISE* photometry of candidate Hya02 is affected by a close star, making its photometry and colours unreliable. Hyades T dwarfs from Bouvier et al. (2008) are marked as open triangles. Overplotted as red crosses are ultracool dwarfs with parallaxes from Dupuy & Liu (2012), after removal of metal-poor dwarfs.

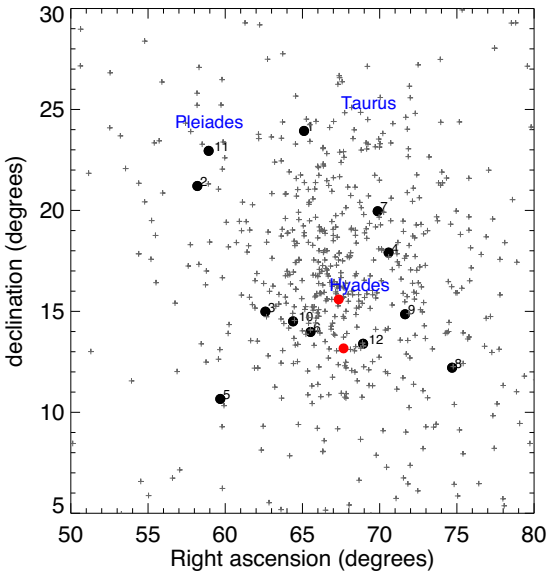

Figure 5. Spatial distribution of the L dwarf candidates from Hogan et al. (2008) with their ID numbers from Table 1 and known members of the Hyades (grey crosses; Goldman et al. 2013). Overplotted as red dots are the two Hyades T dwarfs from Bouvier et al. (2008). The approximate centres of the Pleiades, Taurus, and Hyades regions are also labelled for reference.

(old) ultracool dwarfs with spectral types later than M6 with an rms of 0.4 mag.

For the three late-M dwarfs (Hya01, Hya04, and Hya06), we derive distances of $48.9^{+3.8}_{-3.4}$, $67.1^{+4.7}_{-4.9}$, and $64.3^{+4.5}_{-4.7}$ pc, respectively (Table 2). Assuming a mean distance of 46.34 ± 0.27 pc for the Hyades (Perryman et al. 1998), Hya01 is bona fide member whereas the other two candidates lie slightly further away. However, we cannot discard these objects as members at that stage for several reasons. First, the halo of the Hyades is estimated to be twice the tidal radius (∼10 pc; Perryman et al. 1998; Goldman et al. 2013). Secondly, the typical uncertainty on our spectroscopic distances is of the order of 10 per cent considering our uncertainty of half a subclass on the spectral type to which we should add another 20 per cent error due to the uncertainty of 0.4 mag in the spectral types versus absolute magnitude relation of Dupuy & Liu (2012). Thirdly, we cannot discard the effect of mass segregation due to dynamical evolution for ages older than 600 Myr.

For the L dwarfs, we derive spectroscopic distances in the range 57–67 pc, suggesting that most candidates lie roughly at the distance of the Hyades. The only two exceptions are Hya09 and Hya10 which lie further than 70, $73^{+5.5}_{-7.9}$ and $82.6^{+6.8}_{-6.6}$ pc, respectively (Table 2) but, again, we cannot discard these objects as members at this stage as pointed out above. We classify L dwarfs within the halo of the Hyades as members ('Yes') while the other remain possible members ('Y?', Table 2). This effect might be a result of the dynamical evolution suffered by the cluster (e.g. Vesperini & Heggie 1997; Lamers, Baumgardt & Gieles 2010). However, we caution that our interpretation is based on absolute magnitude–spectral type relationships valid for field dwarfs, which might not be adequate because the Hyades cluster is on average younger than typical nearby ultracool dwarfs.

We note that the two candidates from Hogan et al. (2008) classified as M3 (Hya07) and M5 (Hya05) dwarfs would lie at distances of ∼169–226 and ∼390–560 pc. They lie clearly beyond the Hyades cluster and are background contaminants.

We applied the same absolute magnitude versus spectral type relationship to the two T dwarf members proposed by Bouvier et al. (2008). We inferred spectroscopic distances of 28.8 ± 0.3 pc and 55.5 ± 0.4 pc for CFHT-Hy-20 and CFHT-Hy-21, respectively, based on their *J*-band photometry. These estimates would place those T dwarfs within the halo of the Hyades assuming a mean distance of 46 pc (Perryman et al. 1998). The difference in *J*-band absolute magnitude between a field L3 dwarf and a T1 dwarf is about 2 mag (e.g. Dupuy & Liu 2012), suggesting these T dwarfs

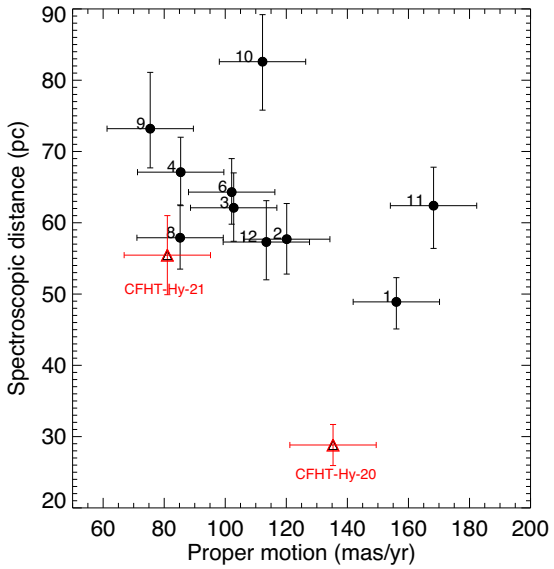

Figure 6. Spectroscopic distances (pc) versus total proper motion (mas yr^{-1}) for the Hyades L (black filled dots with their ID numbers from Table 1) and T (red open triangles) dwarfs. Error bars of 14 mas yr^{-1} are assumed for the total proper motion whereas uncertainties on the spectroscopic distances are from Table 1.

as bona fide members of the Hyades cluster. We suggest to initiate a parallax program on the Hyades L and T dwarfs to place a more reliable constraint on their distance.

We should point out that distance might has an important bearing on the proper motion because an object at the back of the cluster (d ∼60 pc) as opposed to the front (d ∼30 pc) would have a noticeably smaller motion. In Fig. 6, we display the spectroscopic distances as a function of the total proper motion for the spectroscopic L dwarfs and the two Hyades T dwarfs. The typical error bars of the proper motion in each axis derived from the cross-match between the UKIDSS GCS and 2MASS are of the order of 10 mas yr^{-1} (Lodieu et al. 2007), in agreement with the values of ± 7 mas yr^{-1} reported by Hogan et al. (2008). The same uncertainty is used for the T dwarfs (Bouvier et al. 2008). The typical uncertainties on the spectroscopic distances are ∼10 per cent. We observe a linear relation defined by 7/8 of the 10 L dwarfs, (Hya01–09 and Hya12, possibly Hya11 as well) which might argue against cluster membership for Hya10 and one of the two T dwarfs (CFHT-Hy-20; T2).

5.2 Effective temperatures

In the following two subsections, we assume that all candidates are members of the Hyades cluster, except Hya05 and Hya07. We estimated the effective temperatures of the spectroscopic M and L dwarfs in the Hyades, using the mean temperature derived from the spectral type versus effective temperature relations of field L dwarfs presented in Dahn et al. (2002) and Vrba et al. (2004). The coolest L dwarf is Hya12 with an effective temperature below 2000 K. We assumed that these relationships are valid for old field L dwarfs are applicable to the Hyades. This assumption is not exactly correct because members of the Hyades have an age of 575–675 Myr while field L dwarfs are expected to be older than 1 Gyr. Luhman (1999) and Luhman et al. (2003) proposed a temperature scale for young brown dwarfs in IC 348, where the difference between 3 Myr-old M dwarfs and their field counterpart is less than 200–400 K. Hence, we do not expect a difference larger than 100 K between old field dwarfs and Hyades members because of the smaller age difference. This estimate is in line with model predictions (Baraffe et al. 1998; Allard et al. 2012). Our adopted effective temperatures are listed in Table 2 and likely represent upper limits. The uncertainties on the temperatures represent the sum in quadrature of the dispersion observed for a given spectral type listed in the tables of Dahn et al. (2002) and Vrba et al. (2004) and our uncertainty of half a subtype on the spectral type.

5.3 Masses

We derived masses for the confirmed Hyades M and L dwarfs using the latest BT-Settl models (Allard et al. 2012). We assumed an age of 625 Myr for the Hyades. We converted the effective temperatures derived from the optical spectral types into masses using the BT-Settl models, taking into account the uncertainties on the temperatures. We list the range in masses in Table 2.

5.4 Lithium

According to theoretical evolutionary models, L dwarfs are either very low mass stars with ages of a few Gyr or brown dwarfs with masses close to the hydrogen-burning mass limit or younger than 1 Gyr (Burrows et al. 1997; Chabrier & Baraffe 2000). The Li element is rapidly destroyed in the interior of stars, on time-scales shorter than ∼150 Myr, and in massive brown dwarfs on time-scales of a few Gyr. Brown dwarfs with masses lower than 0.055–0.060 $M_{\odot}$ do not burn this element in their interiors because their central temperature is not hot enough to produce this fusion reaction (D'Antona & Mazzitelli 1994; Ushomirsky et al. 1998; Chabrier & Baraffe 2000) According to our mass estimates, the majority of our candidates in the Hyades cluster are very low mass stars and hence, we expect that these objects have destroyed their Li content. However, our candidate with the latest spectral type (Hya12; L3.5) has an estimated mass of only 0.054–0.063 $M_{\odot}$, hence it is expected that it has preserved most of its Li. Given the poor signal-to-noise ratio and resolution of our spectrum, we can only impose an upper limit of 1 Å on the absorption induced by the lithium line at 6708 Å.

In order to confirm this claim, we should obtain a higher resolution spectrum with higher signal-to-noise ratio to detect lithium in absorption at 6708 Å and apply the lithium test (Magazzu, Martin & Rebolo 1991; Magazzu, Rebolo & Pavlenko 1992; Rebolo, Martín & Magazzù 1992; Martin, Rebolo & Magazzu 1994). We place the Hyades T dwarfs in the substellar regime with masses in the 0.03–0.04 $M_{\odot}$ range, estimates slightly lower than the 0.05 $M_{\odot}$ quoted by Bouvier et al. (2008) using the DUSTY models (Chabrier et al. 2000).

6 THE HYADES MASS FUNCTION

Before discussing the shape of the Hyades (system) mass function, we need to compile a sample of members as complete and unbiased as possible. Goldman et al. (2013) published a sample of 776 members with masses ranging between 2.6 and 0.11 $M_{\odot}$ out to 30 pc from the cluster centre. Our spectroscopic follow-up confirms three late-M (Hya01, Hya04, and Hya06) and two early-L dwarfs (Hya03 and Hya08) with masses between 0.1 and 0.069 $M_{\odot}$ within an circular area centred on (RA, Dec.) = (67, 12) deg and a radius of 11 deg (fig. 1 in Hogan et al. 2008). We do not include the other spectroscopic L dwarfs in this discussion because we are unsure about the membership to the Hyades at this stage. We counted 379

Table 3. Number of objects (dN) per mass bin in logarithmic units (dlog (M)) for the Hyades (this work) and Praesepe (Boudreault et al. 2012). Each mass bin has a width of 0.1 in logarithmic space. The last two bins represent the numbers of late-M, L, and T dwarfs most likely members of the Hyades confirmed in this work and Bouvier et al. (2008) whereas the higher mass bins represent members from Goldman et al. (2013) located in the area covered by Hogan et al. (2008).

dlog ($M_{\rm mean}$)	−0.10	−0.30	−0.50	−0.70	−0.90	−1.10	−1.30
d$N_{\rm Hyades}$	101	86 ± 9	87 ± 9	76 ± 9	>31	5–10	>1
d$N_{\rm Prae}$	–	267 ± 11	257 ± 16	255 ± 6	185 ± 16	104 ± 17	>2
d$N_{\rm Prae}$ scaled	–	90 ± 4	87 ± 5	86 ± 2	63 ± 5	35 ± 6	>0.7

sources with masses less than 1 $M_\odot$ in the survey of Goldman et al. (2013) within the 11-deg radius covered by Hogan et al. (2008). We updated the Hyades mass function by adding the five spectroscopically confirmed Hyades members to the sample of Goldman et al. (2013). We estimate our results to be valid for magnitudes brighter than $K \sim 15$ mag, corresponding to masses of 0.05 $M_\odot$ according to the 600 Myr isochrones of the BT-Settl models.

At lower masses, we argue for the membership of one of the T dwarfs (CFHT-Hy-21) reported by Bouvier et al. (2008) whereas the other T dwarf (CFHT-Hy-20) remains as a candidate, as is the latest L dwarf in our sample (Hya12). We do not add a bin in the substellar regime to our revised mass function due to the large uncertainties associated with the membership of the coolest candidates. We should mention that the two T dwarfs from Bouvier et al. (2008) were discovered in an ∼16 deg^2 area with inhomogeneous coverage across the Hyades cluster. These authors argued that there could be 10–15 brown dwarfs down to 0.013 $M_\odot$, although the original population of the cluster may have been of the order of 100–150 prior to the impact of dynamical evolution.

Goldman et al. (2013) presented the Hyades mass function down to 0.11 $M_\odot$, although the last two bins in their fig. 1 4 are incomplete (log (M) = −0.85 and −0.95 with a width of 0.1), corresponding to the sixth column in Table 3. In Table 3, we quote the numbers of members per bin of 0.2 $M_\odot$ in logarithmic units between 1 and 0.1 $M_\odot$ from Goldman et al. (2013) located in the area covered by Hogan et al. (2008). In the log (M) = −1.1 bin, we added the three late-M and two early-L dwarfs confirmed as the most probable Hyades members. This is likely a lower limit (arrow in Fig. 7) because some of the spectroscopic L dwarfs reported in this work might turn out to be members once we have collected additional data. If we include all 10 late-M and early-L dwarfs, the upper limit of the second lowest mass bin would still lie below the field mass function. We have only considered CFHT-Hy-21 in the last bin (log (M) = −1.3, Table 3) but it should be seen as a lower limit mainly because the area covered by Bouvier et al. (2008) is much smaller than the other two surveys considered in our analysis (arrow in Fig. 7). To conclude, we should highlight that the shape of the Hyades substellar mass function still remains to be determined with much better accuracy. Moreover, we emphasize that we do not correct the mass bins for binaries and point out that our analysis makes use of different catalogues coming from surveys with distinct depths and completeness.

Bearing in mind the aforementioned caveats, we compare the Hyades mass function to Praesepe (Table 3; Fig. 7), as published by Boudreault et al. (2012) from a photometric and astrometric survey using the UKIDSS GCS comparable to the study of Goldman et al. (2013). The last bin of the Praesepe mass function is highly incomplete and represents a lower limit, although we note that we have now confirmed spectroscopically an L dwarf member with GTC/OSIRIS (UGCS J084510.66+214817.1 (L0.3 ± 0.4);

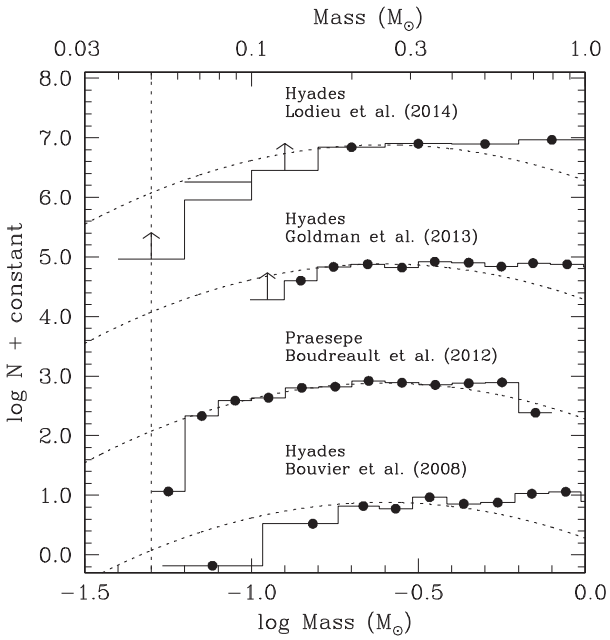

Figure 7. Hyades mass function (number of objects per interval of mass in logarithmic units; lower limits represented as arrows or two horizontal bars in the case of the second lowest mass bin) derived from this work, combining the results of Goldman et al. (2013) with our spectroscopic follow-up. For comparison, we show the mass function of Praesepe (bottom) derived from the photometric and astrometric analysis of the UKIDSS GCS (Boudreault et al. 2012), the original mass functions of Goldman et al. (2013) and Bouvier et al. (2008). Overplotted as a dashed line is the field mass function (Chabrier 2005). We normalized all the MFs to the lognormal fit of Chabrier (2005) at ∼0.3 $M_\odot$ (log (M) ∼ −0.5). The vertical dashed line represents the completeness limit of our work.

Boudreault & Lodieu 2013). The last row in Table 3 quotes the number of objects for Praesepe scaled to the Hyades mass function (d$N_{\rm Prae}$ scaled) around log (M) = −0.5, which corresponds to the peak in the field mass function (Chabrier 2003, 2005). We find that the number of Hyades members (5–10) in the mass bin centred on 0.08 $M_\odot$ is lower than the values of Praesepe (∼3σ or more), a possible result of dynamical evolution. We note that the last bin cannot be directly compared because the UKIDSS GCS survey of Boudreault et al. (2012) is not sensitive to late-L and T dwarfs in Praesepe and the survey by (Bouvier et al. 2008) probes a very small area of the Hyades.

7 CONCLUSIONS

We have presented a photometric, astrometric, and spectroscopic follow-up of 12 L dwarf candidates in the Hyades cluster

announced by Hogan et al. (2008). We have also presented mid-infrared photometry from *WISE* for all L dwarf candidates and the two previously-published T dwarfs. We can summarize the main results of our study as follows.

(i) We classify optically three L dwarf candidates as late-M dwarfs (Hya01, Hya04, and Hya06) with spectral types between M8.5 and M9.5, which are bona fide members of the Hyades cluster.

(ii) We confirm the L dwarf status of seven candidates, with spectral types in the L0–L3.5 range, two of them being very likely members of the Hyades Hya03 and Hya08. Our GTC OSIRIS optical spectra of these Hyades L dwarf members represent spectral templates at an age of 625 Myr, which will we make publicly available to the community.

(iii) We classify the remaining two candidates as M3 (Hya07) and M5 (Hya05), rejecting them as Hyades members.

(iv) We find infrared excesses in four L dwarfs (Hya02, Hya09, Hya11, and Hya12) confirmed spectroscopically, which are typical of young L dwarfs. This result suggests that these objects might belong to younger star-forming regions like Taurus or the Pleiades cluster or these features extent to the age of the Hyades cluster.

(v) We estimate spectroscopic distances of 50–90 pc for the seven candidates confirmed spectroscopically as L dwarfs (Hya02, Hya03, Hya08–12), using the latest absolute *J*-band magnitude versus spectral type relationship of nearby ultracool dwarfs.

(vi) We derive effective temperatures in the range 1980–2420 K, based on the spectral type versus temperature relation of nearby old field dwarfs.

(vii) We infer masses in the 0.08–0.054 $M_{\odot}$ from the latest BT-Settl models, assuming an age of 625 Myr for the Hyades L dwarfs, placing the coolest object below the stellar/substellar boundary if a true member of the cluster.

(viii) Our mass function is in line with a possible deficit of very low mass stars and brown dwarfs in the Hyades, an effect likely due to dynamical evolution.

The original selection of Hogan et al. (2008) was made in a large area covered by an early data release of the UKIDSS GCS but limited by the 2MASS depth, reaching $K \sim 15$ mag. We aim at extending this search to look for fainter and cooler L and T dwarfs in two ways. On the one hand, we plan to cross-match *WISE* with the UKIDSS GCS *K*-band survey to exploit the full depth of 15.5. mag of the *WISE* *w*2 band and the 100 per cent completeness of the GCS down to $K \sim 18$ mag (Lodieu et al., in preparation). On the other hand, we will complement that search by cross-correlating the UKIDSS GCS *K* band with the upcoming UKIRT Hemisphere Survey *J*-band observations whose depth is similar to the UKIDSS Large Area Survey (Dye et al. 2006; Warren et al. 2007), as we did for the Pleiades (Lodieu et al. 2012b), α Persei (Lodieu et al. 2012a), and Praesepe (Boudreault et al. 2012) clusters. Moreover, a moderate-resolution spectroscopic survey should be carried out to investigate the radial velocity of the L dwarf confirmed spectroscopically whose distances lie at the lower and upper limits of the tidal radius of the Hyades cluster. These observations will complement the high precision that the *Gaia* mission will provide down to a spectral type of ∼M8 in the Hyades (de Bruijne 2014).

ACKNOWLEDGEMENTS

NL was funded by the Ramón y Cajal fellowship number 08-303-01-02 and the national program AYA2010-19136 funded by the Spanish ministry of Economy and Competitiveness (MINECO). NL thanks José Acosta Pulido for his help and support with the data reduction of the LIRIS data sets. VJSB is funded by the MINECO project AYA2010-2053. We thank Bartosz Gauza for his help with the Osiris observations. NL thanks Paul Dobbie and Nigel Hambly for valuable comments on the original version of the paper.

This work is based on observations made with the Gran Telescopio Canarias (GTC), operated on the island of La Palma in the Spanish Observatorio del Roque de los Muchachos of the Instituto de Astrofísica de Canarias under CAT programmes GTC27-13B and GTC65-13B.

Based on observations made with the WHT operated on the island of La Palma by the Isaac Newton Group in the Spanish Observatorio del Roque de los Muchachos of the Instituto de Astrofísica de Canarias under the CAT programme 158-WHT38/13B.

This research has made use of the Simbad and Vizier (Ochsenbein, Bauer & Marcout 2000) data bases, operated at the Centre de Données Astronomiques de Strasbourg (CDS), and of NASA's Astrophysics Data System Bibliographic Services (ADS).

GAIA (Graphical Astronomy and Image Analysis Tool) is a derivative of the SKYCAT catalogue and image display tool, developed as part of the Very Large Telescope project at European Southern Observatory. SKYCAT and GAIA are free software under the terms of the GNU copyright.

REFERENCES

Allard F., Homeier D., Freytag B., 2012, Phil. Trans. R. Soc. A, 370, 2765
Allen P. R., Koerner D. W., McElwain M. W., Cruz K. L., Reid I. N., 2007, AJ, 133, 971
Baraffe I., Chabrier G., Allard F., Hauschildt P. H., 1998, A&A, 337, 403
Bastian N., Covey K. R., Meyer M. R., 2010, ARA&A, 48, 339
Bertin E., Arnouts S., 1996, A&AS, 117, 393
Bochanski J. J., West A. A., Hawley S. L., Covey K. R., 2007, AJ, 133, 531
Boesgaard A. M., Friel E. D., 1990, ApJ, 351, 467
Boudreault S., Lodieu N., 2013, MNRAS, 434, 142
Boudreault S., Lodieu N., Deacon N. R., Hambly N. C., 2012, MNRAS, 426, 3419
Bouvier J. et al., 2008, A&A, 481, 661
Burrows A. et al., 1997, ApJ, 491, 856
Casewell S. L., Jameson R. F., Burleigh M. R., 2008, MNRAS, 390, 1517
Casewell S. L., Littlefair S. P., Burleigh M. R., Roy M., 2014, MNRAS, 441, 2644
Cayrel de Strobel G., Crifo F., Lebreton Y., 1997, in Bonnet R. M. et al., eds, ESA SP-402: Hipparcos - Venice '97. ESA, Noordwijk, p. 687
Cepa J. et al., 2000, in Iye M., Moorwood A. F., eds, Proc. SPIE Conf. Ser. Vol. 4008, Optical and IR Telescope Instrumentation and Detectors. SPIE, Bellingham, p. 623
Chabrier G., 2003, PASP, 115, 763
Chabrier G., 2005, in Corbelli E., Palla F., Zinnecker H., eds, in Astrophysics and Space Science Library, Vol. 327, The Initial Mass Function 50 Years Later. Springer-Verlag, Berlin, p. 41
Chabrier G., Baraffe I., 2000, ARA&A, 38, 337
Chabrier G., Baraffe I., Allard F., Hauschildt P., 2000, ApJ, 542, 464
Covey K. R. et al., 2007, AJ, 134, 2398
Cutri R. M. et al., 2003, The IRSA 2MASS All-Sky Point Source Catalog (http://irsa.ipac.caltech.edu/applications/Gator/)
D'Antona F., Mazzitelli I., 1994, ApJS, 90, 467
Dahn C. C. et al., 2002, AJ, 124, 1170
de Bruijne J. H. J., 2014, in Smart R., Barrado D., Faherty J., eds, Proc. GREAT-ESF Workshop, Gaia and the Unseen - the Brown Dwarf Question, Memorie della Societa' Astronomica Italiana (SAIt), preprint (arXiv:1404.3896)
Dobbie P. D., Kenyon F., Jameson R. F., Hodgkin S. T., Hambly N. C., Hawkins M. R. S., 2002, MNRAS, 329, 543
Dupuy T. J., Liu M. C., 2012, ApJS, 201, 19

Dye S. et al., 2006, MNRAS, 372, 1227
Eggen O. J., 1998, AJ, 116, 284
Faherty J. K., Burgasser A. J., Cruz K. L., Shara M. M., Walter F. M., Gelino C. R., 2009, AJ, 137, 1
Gebran M., Vick M., Monier R., Fossati L., 2010, A&A, 523, A71
Gianninas A., Bergeron P., Ruiz M. T., 2011, ApJ, 743, 138
Gizis J. E., Reid I. N., Monet D. G., 1999, AJ, 118, 997
Goldman B. et al., 2013, A&A, 559, A43
Grenon M., 2000, HIPPARCOS and the Luminosity calibration of the Nearer Stars, 24th meeting of the IAU, Joint Discussion, 13 August 2000, Manchester, England, meeting abstract
Hanson R. B., 1975, AJ, 80, 379
Hawley S. L. et al., 2002, AJ, 123, 3409
Høg E. et al., 2000, A&A, 355, L27
Hogan E., Jameson R. F., Casewell S. L., Osbourne S. L., Hambly N. C., 2008, MNRAS, 388, 495
Jameson R. F., Casewell S. L., Bannister N. P., Lodieu N., Keresztes K., Dobbie P. D., Hodgkin S. T., 2008, MNRAS, 384, 1399
Kaiser N. et al., 2002, in Tyson J. A., Wolff S., eds, Proc. SPIE Conf. Ser. Vol. 4836, Survey and Other Telescope Technologies and Discoveries. SPIE, Bellingham, p. 154
Kirkpatrick J. D., Beichman C. A., Skrutskie M. F., 1997, ApJ, 476, 311
Kirkpatrick J. D. et al., 1999, ApJ, 519, 802
Knapp G. R. et al., 2004, AJ, 127, 3553
Kroupa P., 2002, Science, 295, 82
Kroupa P., Weidner C., Pflamm-Altenburg J., Thies I., Dabringhausen J., Marks M., Maschberger T., 2013, The Stellar and Sub-Stellar Initial Mass Function of Simple and Composite Populations. Springer-Verlag, Berlin, p. 115
Lamers H. J. G. L. M., Baumgardt H., Gieles M., 2010, MNRAS, 409, 305
Lawrence A. et al., 2007, MNRAS, 379, 1599
Leggett S. K., Hawkins M. R. S., 1989, MNRAS, 238, 145
Lodieu N., Scholz R.-D., McCaughrean M. J., Ibata R., Irwin M., Zinnecker H., 2005, A&A, 440, 1061
Lodieu N., Hambly N. C., Jameson R. F., Hodgkin S. T., Carraro G., Kendall T. R., 2007, MNRAS, 374, 372
Lodieu N., Deacon N. R., Hambly N. C., Boudreault S., 2012a, MNRAS, 426, 3403
Lodieu N., Deacon N. R., Hambly N. C., 2012b, MNRAS, 422, 1495
Luhman K. L., 1999, ApJ, 525, 466
Luhman K. L., Stauffer J. R., Muench A. A., Rieke G. H., Lada E. A., Bouvier J., Lada C. J., 2003, ApJ, 593, 1093
Maeder A., Mermilliod J. C., 1981, A&A, 93, 136
Magazzu A., Martin E. L., Rebolo R., 1991, A&A, 249, 149
Magazzu A., Rebolo R., Pavlenko I. V., 1992, ApJ, 392, 159
Manchado A. et al., 1998, in Fowler A. M., ed., Proc. SPIE Conf. Ser. Vol. 3354, Infrared Astronomical Instrumentation. SPIE, Bellingham, p. 448
Martin E. L., Rebolo R., Magazzu A., 1994, ApJ, 436, 262
Miller G. E., Scalo J. M., 1979, ApJS, 41, 513
Ochsenbein F., Bauer P., Marcout J., 2000, A&AS, 143, 23
Pancino E. et al., 2012, MNRAS, 426, 1767
Parker R. J., Andersen M., 2014, MNRAS, 441, 784
Perryman M. A. C. et al., 1998, A&A, 331, 81
Rebolo R., Martín E. L., Magazzù A., 1992, ApJ, 389, L83
Reid N., 1992, MNRAS, 257, 257
Reid N., 1993, MNRAS, 265, 785
Reid I. N., Gizis J. E., 1997, AJ, 114, 1992
Reid I. N., Hawley S. L., 1999, AJ, 117, 343
Reid I. N., Kirkpatrick J. D., Liebert J., Gizis J. E., Dahn C. C., Monet D. G., 2002, AJ, 124, 519
Röser S., Demleitner M., Schilbach E., 2010, AJ, 139, 2440
Röser S., Schilbach E., Piskunov A. E., Kharchenko N. V., Scholz R.-D., 2011, A&A, 531, A92
Salpeter E. E., 1955, ApJ, 121, 161
Scalo J. M., 1986, Fundam. Cosm. Phys., 11, 1
Skrutskie M. F. et al., 2006, AJ, 131, 1163
Stauffer J. R., Liebert J., Giampapa M., Macintosh B., Reid N., Hamilton D., 1994, AJ, 108, 160
Stauffer J. R., Liebert J., Giampapa M., 1995, AJ, 109, 298
Thies I., Kroupa P., 2007, ApJ, 671, 767
Thies I., Kroupa P., 2008, MNRAS, 390, 1200
Tody D., 1986, in Crawford D. L., ed., Proc. SPIE Conf. Ser. Vol. 627, Instrumentation in Astronomy VI. SPIE, Bellingham, p. 733
Tody D., 1993, in Hanisch R. J., Brissenden R. J. V., Barnes J., eds, ASP Conf. Ser. Vol. 52, Astronomical Data Analysis Software and Systems II. Astron. Soc. Pac., San Francisco, p. 173
Ushomirsky G., Matzner C. D., Brown E. F., Bildsten L., Hilliard V. G., Schroeder P. C., 1998, ApJ, 497, 253
van Leeuwen F., 2007, A&A, 474, 653
Vesperini E., Heggie D. C., 1997, MNRAS, 289, 898
Vrba F. J. et al., 2004, AJ, 127, 2948
Warren S. J. et al., 2007, MNRAS, 375, 213
Wright E. L. et al., 2010, AJ, 140, 1868
York D. G. et al., 2000, AJ, 120, 1579
Zapatero Osorio M. R., Béjar V. J. S., Miles-Páez P., Peña-Ramírez K., Rebolo R., Pallé E., 2014, A&A, 568, 6

This paper has been typeset from a TEX/LATEX file prepared by the author.